Ultrafast Pump−Probe Studies of Excited-State Charge-Transfer Dynamics in Blue Copper Proteins

Lewis D. Book,[†] David C. Arnett,[‡] Hanbo Hu,[§] and Norbert F. Scherer*,[†]

Department of Chemistry and the James Franck Institute, University of Chicago, Chicago, Illinois 60637, Environmental Molecular Sciences Laboratory, Pacific Northwest Laboratory, Richland, Washington 99352, and Department of Chemistry, University of Pennsylvania, Philadelphia, Pennsylvania 19104-6323

Received: November 19, 1997; In Final Form: January 29, 1998

We report the results of ultrafast pump−probe measurements on three blue copper proteins: spinach plastocyanin, poplar plastocyanin, and human ceruloplasmin. Electronic population dynamics and vibrational coherences involving d → d transitions of the blue copper active site are observed using both wavelength-integrated and wavelength-resolved detection. Depending on the protein and the method of detection, the pump-induced bleaches of the electronic ground state decay with time constants of 230−300 fs. The pump−probe signals are modulated by oscillations that correspond to vibrational coherences induced by the ultrashort pulses. The frequencies of some of these oscillations can be matched with modes observed in resonance Raman studies of these proteins. For spinach plastocyanin and ceruloplasmin, wavelength-resolved signals reveal a previously unreported vibration at ∼500 cm^{-1} whose decay dynamics are consistent with the excited-state lifetime. The origin of this mode is argued to result from Duschinsky rotation. The relevance of these pump−probe results to the development of a model for biological electron transport in these proteins is discussed.

I. Introduction

A major goal of current research in biophysical chemistry is to understand electron transfer in proteins in terms of Marcus theory.[1,2] This formulation, which has been verified for small molecular systems,[3] gives a rate constant for electron transfer in terms of the free-energy change of the reaction, the coupling between the redox states, and the reorganization energy of nuclear degrees of freedom.[4] Although the role these three quantities play in determining the rate is well understood, it is usually difficult to determine their values in practice. For example, calculation of the reorganization energy requires a knowledge of the coupling strengths of the protein's vibrational modes to the electron-transfer event.[5] It is especially difficult to study the effect of specific protein modes on dynamics in thermally activated electron-transfer reactions because of the separation of time scales between molecular vibrations (femtoseconds) and electron-transfer rates (milliseconds to microseconds).[2a] For this reason, it is useful to study photoinduced charge-transfer processes that can be triggered by short optical pulses, even if the charge-transfer process that occurs is not precisely equivalent to a physiological electron transfer.[1a]

Blue copper proteins function as mobile electron carriers in a wide variety of biological systems.[6,7] The "type I" active sites of these proteins consist of a single copper atom ligated to four or five amino acid side chains in a distorted tetrahedral or trigonal-bipyrimidial geometry. For example, in the active site of plastocyanin, the copper atom is ligated to a sulfur atom from a cysteine residue, two nitrogens from histidine residues, and another sulfur atom from a methionine residue.[5] In oxidized

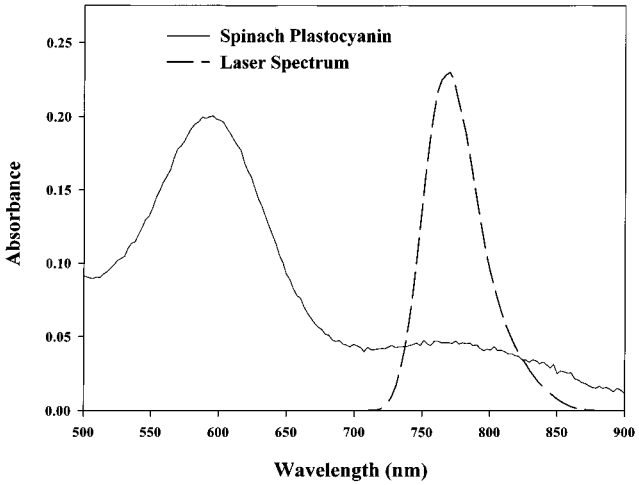

Figure 1. Absorption spectrum of spinach plastocyanin and the laser spectrum used in the pump−probe measurements. The absorption band at ∼600 nm is the ligand-to-metal charge-transfer transition, while the band centered at ∼770 nm is a combination of three d → d transitions of the blue copper atom.

form, optical absorption spectra of plastocyanin and other blue copper proteins show two broad peaks centered at 600 and 770 nm (Figure 1). The stronger peak at 600 nm ($\epsilon \approx 5000$ M^{-1} cm^{-1}), which is the source of the blue color, has been identified formally as a ligand-to-metal charge-transfer transition between the cysteine sulfur ligand and the copper center.[8] Semiempirical electronic-structure calculations have indicated, however, that little charge redistribution actually occurs in this transition, so this characterization may be misleading.[9,10] The weaker peak at 770 nm is a combination of three transitions from filled copper d orbitals to the half-filled $d_{x^2-y^2}$ orbital (Figure 2; the coordinate system follows that of ref 8). These symmetry-forbidden

* To whom correspondence should be addressed.
[†] University of Chicago.
[‡] Pacific Northwest Laboratory.
[§] University of Pennsylvania.

S1089-5639(98)00263-1 CCC: $15.00
Published on Web 04/11/1998

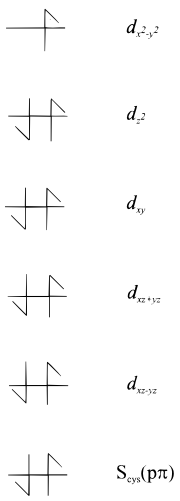

Figure 2. Relative energy ordering of the highest occupied orbitals in blue copper proteins. The ground-state configuration of the copper atom d levels and the S(cysteine) orbital involved in visible transitions are shown. The level spacings are not drawn to scale.

transitions borrow intensity from the charge-transfer transition. Circular dichroism measurements have resolved and identified three different peaks: $d_{xy} \rightarrow d_{x^2-y^2}$ ($\lambda_{max} \approx 925$ nm, $\epsilon \approx 250$ M^{-1} cm^{-1}), $d_{xz+yz} \rightarrow d_{x^2-y^2}$ (780 nm, 1400 M^{-1} cm^{-1}), and $d_{xz-yz} \rightarrow d_{x^2-y^2}$ (715 nm, 500 M^{-1} cm^{-1}). The $d_{z^2} \rightarrow d_{x^2-y^2}$ transition is not optically active. The widths of the three resonances are all quite broad; each is about 2000 cm^{-1} fwhm.[11]

The most widely studied blue copper protein is plastocyanin, a small (10.5 kDa) photosynthetic protein of plants, algae, and cyanobacteria that transfers an electron from cytochrome *f* in photosystem II to a chlorophyll in photosystem I.[12] Although a plastocyanin protein contains a single copper center, many proteins in this class contain several copper atoms, some of which may not be bound to active sites of the blue type I configuration. Ceruloplasmin is one such protein, containing six copper atoms, three of which are in type I sites and three of which are coupled in a trinuclear center.[13] This large (132 kDa) protein functions in copper and iron transport, in ferrioxidase, amine oxidase, and antioxidant activity and possibly has other functions.[14]

Blue copper proteins are excellent systems for spectroscopic studies of protein electron transfer. In oxidized form, their electronic transitions in the visible region are accessible by standard continuous wave and pulsed laser systems. The structure of a common blue copper protein, poplar plastocyanin, is well characterized by X-ray crytallography.[12,15] Several complete and partial plastocyanin structures have also been determined by NMR spectroscopy.[12] Ungar, Scherer, and Voth recently developed molecular-mechanics potentials for classical-dynamics simulations on both the ground and charge-transfer states of plastocyanin.[16] They were able to identify internal coordinates that are coupled to the optical transition that connects these states. Some of these vibrations appear to be coupled to protein atomic motions along proposed physiological electronic transport paths. This raises the possibility of connecting information obtained from optical spectroscopic measurements with the actual biological electron-transfer event.

Several groups have performed resonance Raman studies utilizing the charge-transfer transitions ($S_{cys}(p\pi) \rightarrow d_{x^2-y^2}$) of these proteins.[17−20] Observed frequencies in a resonance Raman spectrum correspond to ground-state vibrational modes, while their intensities are related to their strength of coupling to the electronic transition.[21] For plastocyanin, these studies typically reported about eight frequencies coupled to the protein's charge-transfer band: six with frequencies between 370 and 480 cm^{-1} assigned to the Cu−S(cysteine) stretch mixed into several normal modes, a mode at 760 cm^{-1} assigned to the C−S stretch of the cysteine residue, one at around 260 cm^{-1} corresponding to Cu−N(histidine) stretches, and a broad combination band at around 800 cm^{-1}. It has been suggested that the last band is evidence of significant Duschinsky rotation in the excited state.[17a] Similar results were obtained for ceruloplasmin.[17a] The fact that most of the resonance-enhanced modes involve the Cu−S(cysteine) stretch can be rationalized from the results of semiempirical calculations, which show that the electronic excitation is localized around this bond.[9,10] Thus, it is expected that this bond will undergo the most distortion upon excitation.[16] Solomon et al. have suggested that the Cu−S(cysteine) bond plays a key role in the physiological electronic-transfer event.[7]

Loppnow and co-workers have made measurements of absolute resonance Raman cross sections for parsley, spinach, and poplar plastocyanins.[20] They estimated the total mode-specific reorganization energy upon excitation for all three species to be 0.18 ± 0.01 eV, although significant species-to-species differences were found among the reorganization energies of individual modes. For parsley plastocyanin, the contribution of the low-frequency protein "solvent" modes to the reorganization energy was estimated to be 0.06 eV. Using measurements of the fluorescence quantum yield and the radiative rate constant, they estimated the lifetime of the charge-transfer state to be 20 ± 15 fs.

Resonance Raman measurements have yielded a substantial amount of data on vibrational dynamics that will be useful in forming an accurate description of electron transfer in blue copper proteins. However, this method cannot give a complete picture of certain processes relevant to this problem, such as the nature of nuclear dynamics in excited states and the couplings among the protein's electronic levels. This information is needed because lower-level excited states serve as acceptor levels when the protein receives an electron from a redox partner. Certain time-resolved optical techniques give spectroscopic information that is complementary (but not identical) to that obtained from frequency-domain resonance Raman.[22] For example, in a resonant pump−probe experiment, a pump pulse perturbs the sample, creating population in the excited electronic state and vibrational coherences in the both the ground and excited states. A delayed probe pulse then interrogates the sample and is attenuated, transmitted, or amplified by the sample before it reaches a detector. Positive contributions to the signal (in the conventions repeated in the figures below) result from bleaching of the ground state and stimulated emission from the excited state, while negative contributions come from transient absorption by the excited state or other photoproducts. Oscillatory components reflect vibrational coherences that can be induced in both the ground and excited states. Under many circumstances, the pump−probe signal can be detected for any probe delay time until the system has returned to its ground equilibrium state. This is in contrast to resonance Raman, where the time scale of the measurement cannot be experimentally controlled.

Beck and co-workers recently performed pump−probe measurements on the charge-transfer transition of spinach plastocyanin.[23] They determined that the charge-transfer state decays by a hole transfer process with a 125-fs lifetime into an excited d state, which in turn converts to the ground-state configuration with a time constant of 285 fs. Their estimate of the lifetime of the charge-transfer state is several times greater than that

made by Loppnow's group.[20a] From transient pump−probe spectra Beck and co-workers determined that fast intramolecular vibrational redistribution and/or protein−matrix solvation occurs in the charge-transfer state on a time scale shorter than the lifetime of the state. Owing to the length (∼80 fs) of the optical pulses used in this study, it was not possible to produce vibrational coherences for modes coupled to the electronic excitation.

The d → d transitions of blue copper proteins ($\lambda_{max} \approx 770$ nm) overlap the spectrum of self-mode-locked titanium:sapphire lasers (see Figure 1).[24,25] These lasers routinely produce pulses 10−20 fs in duration, short enough in principle to time-resolve all modes that have been observed in resonance Raman studies of blue copper proteins. This paper reports vibrationally impulsive, time-resolved pump−probe measurements of three of these proteins: spinach plastocyanin, poplar plastocyanin, and ceruloplasmin. The observations of nuclear and electronic relaxation associated with optical excitation are related to prior resonance Raman and pump−probe results. Unique vibrational frequencies are observed and attributed to excited-state modes that differ from the ground state by Duschinsky rotation. Further experimental and theoretical work that is needed to better understand electron transfer in blue copper proteins is discussed. Preliminary accounts of this work have been published elsewhere.[26]

II. Experimental Section

Protein Samples. Spinach plastocyanin was isolated from spinach leaves according to the procedure described by Morand and Krogmann.[27] The sample was concentrated to ∼0.5 mM in a centrifuge using an Amicon centriprep-3 unit and stored in the dark at 0° C until used. To ensure that all proteins were oxidized, a drop of 1 mM potassium ferricyanide was added to the 3−5 mL sample volume. A poplar plastocyanin sample was kindly provided by Professor Glen Loppnow.[20a] Human ceruloplasmin was obtained from Sigma in a buffer solution of about 0.3 mM. The concentration of this solution was doubled with a centriprep-3 unit before usage.

Ultrafast Pump−Probe Setup. The femtosecond spectrometer is based on a home-built, cavity-dumped Ti:sapphire laser that is described in detail in other publications.[25] The experiments described in this paper employ 30−50 nJ pump pulses of ∼16 fs fwhm (at the sample) centered at 770 nm at repetition rates of 250−500 kHz. After exiting the cavity, the beam is sent through a prism pair to compensate for residual chirp on the pulse and to precompensate for dispersion due to the beam splitter, compensating plate, focusing lens, and front sample-cell window. The pulse train is next split into pump and probe beams with an intensity ratio of 4:1. The probe pulse is sent down a precision-moving delay line (Melles-Griot Nanomover) that allows the time difference between the arrival of the pump and probe pulses at the sample to be scanned. Both beams are focused with a 10-cm focal length diode doublet lens into the sample, which is contained in an airtight, 1-mm path length spinning cell rotating at approximately 20 Hz. The beams are recollimated after passing through the sample and then directed toward an aperture that allows the probe beam to pass but blocks the pump. For wavelength-integrated measurements, the probe beam is attenuated with neutral-density filters and detected with a photomultiplier tube (Hamamatsu R928) and amplified (Centronic PA-100). This signal is analyzed by a digital lock-in amplifier (Stanford Research Systems 830) referenced to a chopper modulating the pump beam and then is stored in an IBM-compatible computer. Wavelength-resolved measurements are performed by dispersing the probe beam in a 0.25-m monochromator (CVI) with a 2-nm spectral window. The signal at a selected wavelength is detected with an avalanche photodiode (Advanced Photonics) and then amplified and analyzed in the same fashion as the integrated signal.

The instrument response function was determined as the pump−probe cross correlation using background-free second-harmonic generation in a 100-mm thick KDP crystal placed in the sample position. Also, nonresonant pure-solvent pump−probe transients were recorded to aid in the analysis of the protein pump−probe signals near time zero. Absorption spectra of the blue copper protein samples were taken immediately before and immediately after the ultrafast measurements to see if any photodegradation of the samples had occurred. The ratio of the absorption peak height at 600 nm to the peak height at 278 nm (amino acid absorption) changed little (<5%), indicating that little photodegradation took place.

III. Results

Figure 3a shows the wavelength-integrated pump−probe measurement for spinach plastocyanin. The dots in the figure represent experimental data, while the line is a fit, which is explained below. The signal decays from a positive value (pump-induced probe transmission) to a baseline with weakly superimposed oscillations. The large-amplitude feature around the zero-of-time that goes off scale (but is seen in the inset) is the nonresonant absorption of the buffer solution. Although the solvent contribution masks the protein signal for delay times when the pump and probe pulses are overlapped, this instantaneous response quickly gives way to a signal completely due to the protein sample. The inset in Figure 3a shows the pump−probe signal using a scale that displays the entire pump−probe response; this plot shows that the protein response dominates the signal except for delay times less than ∼75 fs. This plot can be compared with that in Figure 3b, which shows the pump−probe signal of a buffer solution containing no protein, that is, the solvent-only response. This buffer-only waveform shows the prominent antisymmetric shape around the zero-of-time but has no amplitude (or oscillations) beyond the overlap of the pump and probe pulses.

At a probe delay time just after the buffer response had ceased, the plastocyanin pump−probe signal was fit to a sum of a decaying exponential and a constant offset; parameters are listed in Table 1. The decaying exponential (time constant of 280 fs) accounts for 98.3% of the initial fit amplitude, while the constant offset takes up the remaining 1.7%. This fit was subtracted from the data to produce residuals that contain the vibrational character of the signal. This oscillatory waveform was analyzed in the time and frequency domains by linear-prediction singular-value decomposition[28] (LPSVD) and Fourier transformation, respectively. The LPSVD analysis yields the frequency, amplitude, phase, and exponential time constant for a series of cosine functions "fitting" the data (see Figure 4b for a typical fit). It should be understood that an LPSVD time constant determined from experimental data will be a lower limit for the time constant of the component, especially for components of small amplitude. The reason for this is that once the amplitude of an oscillation has decayed below the noise level, the LPSVD routine assumes it to have completely decayed. The most prominent oscillation is found to have a frequency of 372 cm^{-1} and a decay constant of 1.44 ps (Table 1). The residuals were also Fourier transformed and deconvoluted with the instrument response function to determine the oscillatory frequencies present, which are given in the Fourier absolute

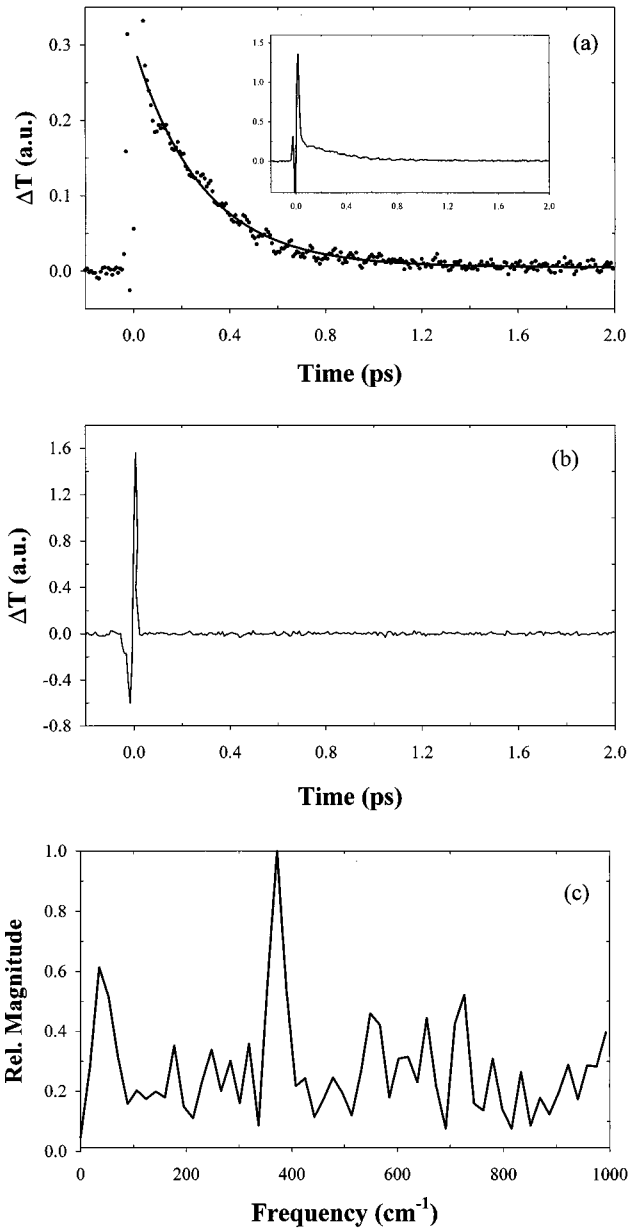

Figure 3. (a) Wavelength-integrated pump−probe signal for spinach plastocyanin. Dots are the experimental data, and line is an exponential fit (see text). The inset shows the same data on a scale that allows the entire buffer response to be seen. (b) Wavelength-integrated pump−probe signal for the pure buffer solution. (c) Fourier absolute magnitude spectrum of the oscillatory components present in the integrated pump−probe signal of spinach plastocyanin. This spectrum is obtained by the subtraction of an exponential fit and a constant offset from the time-domain data followed by Fourier transformation of the residual.

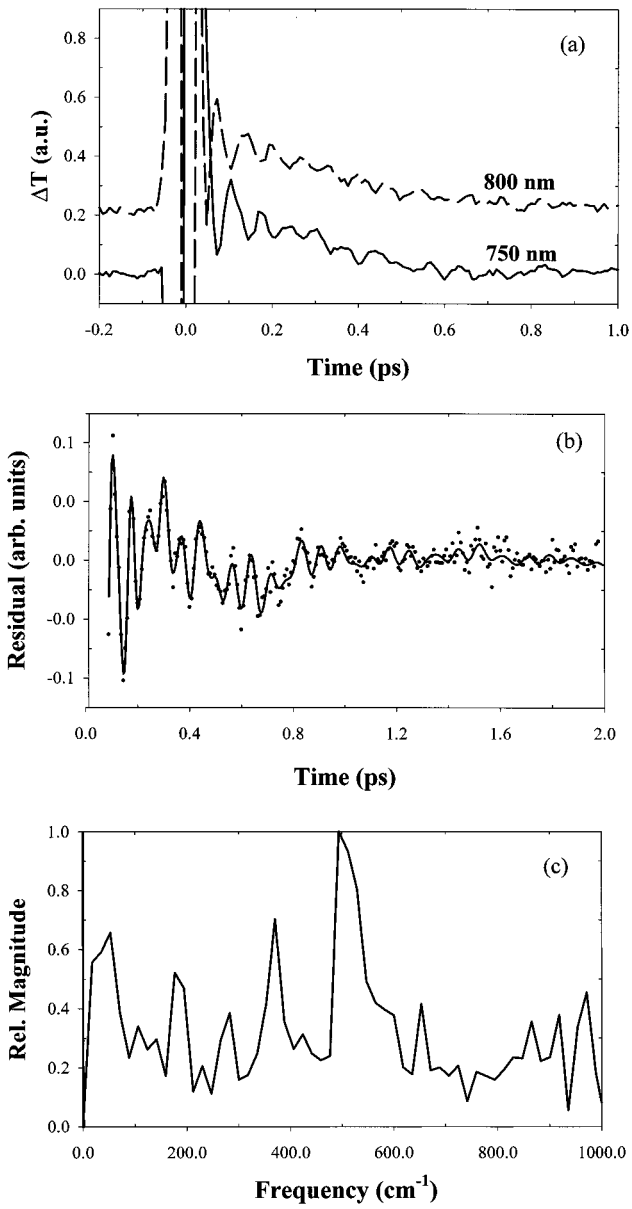

Figure 4. (a) Wavelength-resolved pump−probe signals for spinach plastocyanin with detection at 750 and 800 nm. (b) LPSVD fit (line) to the residual of 750-nm signal (dots) following subtraction of an exponential fit. (c) Absolute spectrum of the oscillatory components present in the 750-nm wavelength-resolved pump−probe signal of spinach plastocyanin.

magnitude spectrum in Figure 3c. The two most prominent features in this spectrum are at 372 and 35 cm^{-1}.

Figure 4a shows wavelength-resolved pump−probe signals of spinach plastocyanin for detection at 750 and 800 nm. These signals have exponential decay times on the same time scale as that of the integrated measurement (Table 1) and also have small constant offsets of 0.7% (750 nm) and 1.1% (800 nm). However, detection to the blue of the laser center frequency gives a somewhat faster decay time, while detection to the red gives a slightly slower time constant than in the case of the wavelength-integrated signal. Such a response is consistent with excited-state vibrational relaxation or solvation detected by stimulated emission but opposite that expected for ground-state thermalization. Furthermore, both traces have much more oscillatory character than the integrated signal. Note that the major oscillation in the 750-nm signal is phase-shifted by 180° relative to that in the 800-nm signal. Figure 4b shows the LPSVD fit to the 750-nm residuals with oscillations at 42, 166, 250, 367, and 510 cm^{-1}. The last mode has a decay time of 260 fs. Such a mode is not present in the wavelength-integrated data. The 166 cm^{-1} feature may be a beat frequency between the intense modes at 367 and 510 cm^{-1}, while the 250 cm^{-1} feature is consistent with the Cu−N(histidine) stretching frequency. Fourier absolute magnitude spectra of the oscillations in these signals are strikingly different from the integrated spectrum. The wavelength-resolved spectra exhibit a broad, intense feature centered at 510 cm^{-1} (Figure 4c shows the spectrum for 750-nm detection) and weaker bands at 53, 172, 277, and 367 cm^{-1}.

The wavelength-integrated pump−probe signal and the corresponding absolute spectrum for poplar plastocyanin (Figure

TABLE 1: Time Constants for the Decay of the Pump-Induced Ground-State Bleach/Excited-State Stimulated Emission in Spinach Plastocyanin, Poplar Plastocyanin, and Human Ceruloplasmin[a]

blue copper protein	pump−probe measurement	frequency (cm^{-1})	time constant (fs)
spinach plastocyanin	integrated	0	280
		372	1440
	WR 750 nm	0	230
		250	570
		510	260
	WR 800 nm	0	300
		253	530
		505	265
poplar plastocyanin	Integrated	0	280
		385	2520
	WR 750 nm	0	270
		385	1360
	WR 800 nm	0	300
		380	1410
human ceruloplasmin	integrated	0	260
	WR 750 nm	0	240
		361	560
		506	250

[a] Zero-frequency time constants refer to the exponential fit through the decay. Time constants for high-frequency components refer to modes determined by LPSVD analysis of oscillations that modulate the decay of the induced transparency (see text). The LPSVD routine fits the signal to a function of the form $S(t) = \sum_i [A_i \cos(w_i t + \phi_i) \exp(-t/\tau_i)]$, where the variables have their usual meanings. Parameters are shown for both wavelength-integrated and wavelength-resolved (WR) detection of the pump−probe signal.

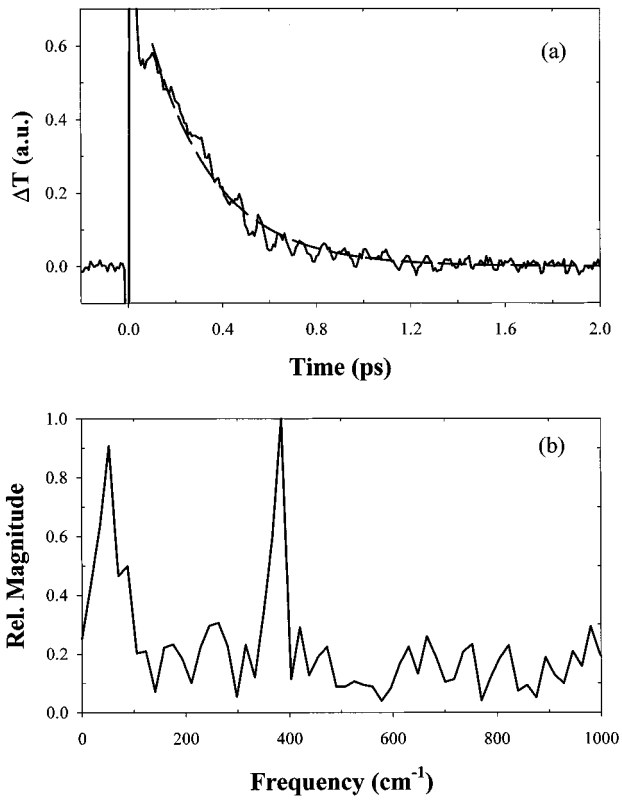

Figure 5. (a) Wavelength-integrated pump−probe signal of poplar plastocyanin. (b) Fourier spectrum of the oscillatory components present in the integrated pump−probe signal of poplar plastocyanin.

5, Table 1) are quite similar to those obtained for the spinach protein. The time-domain signal decays with a time constant of 280 fs, while the spectrum shows prominent oscillations at 385 and 53 cm^{-1}. The 385 cm^{-1} mode decays with a time constant of 2.52 ps. For the poplar signals, adding a constant

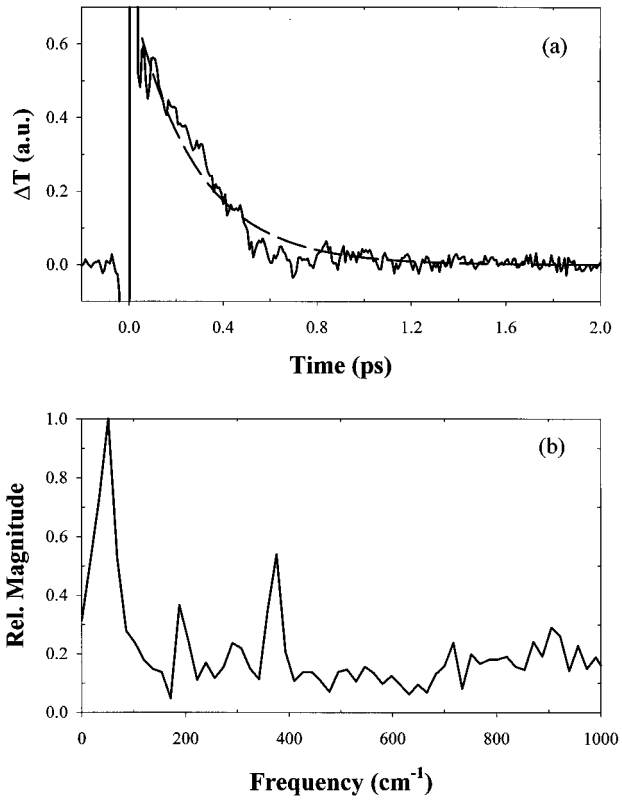

Figure 6. (a) A 750-nm wavelength-resolved pump−probe signal of poplar plastocyanin. (b) Fourier spectrum of the oscillatory components present in the 750-nm wavelength-resolved pump−probe signal of poplar plastocyanin.

offset to the exponential analysis did not noticeably improve the fit. The 750-nm wavelength-resolved pump−probe signal for the poplar protein is shown in Figure 6a. These data contrast sharply with the analogous spinach measurements in that only fairly weak oscillations are present. The Fourier magnitude spectrum (Figure 6b) reveals that the strong mode at ∼500 cm^{-1} observed in spinach plastocyanin is not seen in the poplar data.

Pump−probe results for ceruloplasmin show a closer resemblance to the spinach plastocyanin measurements than they do to the poplar measurements. Like both plastocyanins, the ceruloplasmin wavelength-integrated signal shows little oscillatory character; owing to the noise level, no frequencies could be definitively identified. Still, the exponential decay time of the pump-induced transmission is 260 fs, similar to those of the other two proteins. The 750-nm wavelength-resolved signal shown in Figure 7 is highly oscillatory. Strong Fourier components are observed at 43, 361, 434, and 506 cm^{-1}. The LPSVD decay time for this last mode is 250 fs. Comparison of this spectrum with that of spinach plastocyanin (Figure 4b) shows some common features, although the amplitudes are clearly different.

IV. Discussion

Population Relaxation. In analyzing the pump−probe data for blue copper proteins, it is important to understand which electronic transitions may contribute to the signal. The optical pulses used in the present measurements are centered at 770 nm with a bandwidth of ∼50 nm. The transition with the most oscillator strength in this range is $d_{xz+yz} \rightarrow d_{x^2-y^2}$, although the spectral width of the laser also overlaps with the wings of the two other d → d transitions.[11] Therefore, electronic transitions may originate from up to three ground states to a common excited state (Figure 2). Following excitation, population transfer may occur among these ground states by hole-transfer

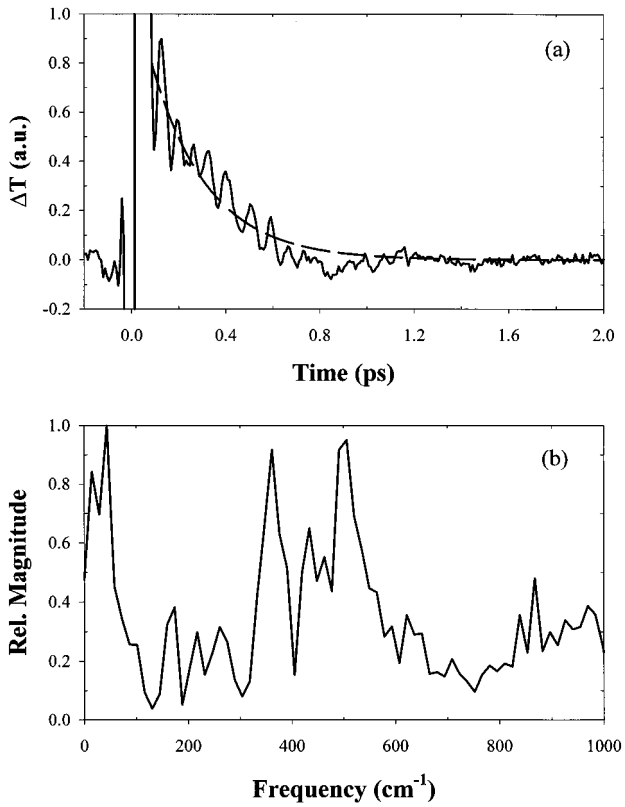

Figure 7. (a) A 750-nm wavelength-resolved pump−probe signal of human ceruloplasmin. (b) Fourier spectrum of the oscillatory components present in the 750-nm wavelength-resolved pump−probe signal of human ceruloplasmin.

processes, in addition to nonradiative relaxation of the excited state.

Pump−probe signals in this study consist of a fast decay modulated by oscillations. The interpretation of the rapidly decaying component is straightforward: most of the excited-state population created by the pump pulse quickly (time constant of <300 fs) returns to the ground state (or states) in a nonradiative fashion. This observation implies that within hundreds of femtoseconds of its creation most of the excited population reaches points in the excited-state phase space that are strongly coupled to a lower state. To the extent that the(se) electronic transition(s) involves the movement of charge from ligand atoms to the copper center, the decay of excited-state population can be considered to occur by a return charge-transfer process. Because these absorptions borrow intensity from the 600-nm "charge-transfer" band, it may be reasonable to assume that a charge-transfer process is being observed. However, this interpretation must be viewed with caution, since semiempirical electronic-structure calculations have suggested that little or no net charge redistribution actually occurs in the formal charge-transfer transition.[9,10] Nevertheless, a nonradiative relaxation process (internal conversion) is occurring, since the oscillator strength of the band is too small to cause radiative relaxation on this time scale.

The wavelength-integrated pump−probe signal for spinach plastocyanin indicates that the excited-state population created by the pump pulse returns to the ground state with a time constant of 280 fs. This result is in excellent agreement with the work of Beck and co-workers, who performed pump−probe measurements using plastocyanin's 600-nm charge-transfer transition.[23] They report that the charge-transfer ($S_{cys}(p\pi) \rightarrow d_{x^2-y^2}$) excitation decays via hole transfer to the d_{xz+yz} orbital, which then returns to the ground-state configuration in a process that has a time constant of 285 fs. Since 770-nm pulses primarily excite population from the d_{xz+yz} level, the present measurements directly probe the decay process that is the second part of a two-step decay of the charge-transfer excitation.

The addition of a small offset (<2% of the initial fit amplitude) just above the noise level significantly improved the fit to the spinach plastocyanin pump−probe signals. The offset appears stationary on the time scale of the measurement and therefore must decay with a time constant greater than several picoseconds. This feature could be a result of a small amount of population becoming trapped on the excited-state surface, preventing the reestablishment of equilibrium on the few-picosecond time scale. For example, some excited population could move into a region of the potential-energy surface that is only weakly coupled to any lower state. Alternatively, the nonradiative couplings between the ground state and that of the weaker d → d transitions could be substantially smaller than that of the $d_{xz+yz} \rightarrow d_{x^2-y^2}$ transitions. A small amount of excited population created from the weaker transitions might have a significantly longer lifetime. Another possibility can be envisioned by picturing (Figure 2) the excited state created by a $d_{x^2-y^2} \rightarrow d_{xz+yz}$ absorption. In this configuration, partial energy relaxation could occur by the movement of an electron (hole) from the d_{xy} or d_{z^2} orbitals to the d_{xz+yz} orbital (d_{xz+yz} to d_{xy} or d_{z^2}). A "cascade" effect like this could greatly increase the time required for the system to return to its equilibrium ground-state configuration. This offset could also be a result of a nonequilibrium vibrational population distribution in the ground state produced by Raman-like processes or the decay of excited-state population into high-lying vibrational levels of the ground state. Since vibrational coherence relaxation of the 370 cm^{-1} mode occurs on a time scale greater than a picosecond, vibrationally excited ground-state modes could induce a transparency that persists beyond the range of our measurements.

Referring to Table 1, note that the time constants for the 750-nm wavelength-resolved measurements are all smaller than the corresponding wavelength-integrated time constants, while those for 800-nm detection are larger. This effect could be an indication of vibrational-energy relaxation or solvation within the electronic excited-state surface. For example, vibrational cooling takes place in the excited state as the initial wave packet created by the pump pulse relaxes from a coherent superposition to a thermal distribution. As vibrational population relaxation occurs, the average energy for transitions from the excited surface to the ground state decreases. This effectively decreases the decay time of the stimulated-emission component of the pump−probe signal for wavelengths to the blue of the laser center frequency while increasing the decay time for wavelengths to the red of the center frequency. Another form of energy relaxation can occur if the excited active site is "solvated" by the protein; that is, the (free) energy of the excited state is lowered relative to the ground state by reorganization of the surrounding environment. This effect is responsible for the dynamic Stokes shift observed in time-resolved fluorescence studies of the solvation of chromophores in liquid solution.[29] As explained in ref 29b, the magnitude of the dynamic Stokes shift is strongly dependent on the extent of charge redistribution in the chromophore upon excitation. Calculations by two groups have suggested that little charge redistribution occurs in blue copper proteins upon optical excitation,[9,10] which may mean protein solvation of the active site is negligable. Energy relaxation due to solvation would have a qualitatively similar effect on wavelength-dependent decay constants as vibrational relaxation. This is because the blue part of the spectrum would

decay while the red portion builds up. A more detailed set of spectrally resolved data would be required to definitively establish whether only vibrational relaxation or also solvation by the protein matrix contributes to the spectral evolution.

Vibrational Coherences. The ~16-fs optical pulses used in these pump−probe measurements allow the production and observation of vibrational coherences with frequencies greater than 800 cm^{-1}. This is enough bandwidth to resolve all vibrations that have been reported in resonance Raman measurements of blue copper proteins, although it is not expected that identical results will be obtained. First, it is important to keep in mind that the resonance Raman studies have probed the blue copper charge-transfer transition, while the present set of measurements accesses the d → d transitions. However, because these latter transitions borrow intensity from the charge-transfer band,[8] it may be expected that the nuclear dynamics coupled to all these electronic transitions will be somewhat similar. Second, Johnson and Myers have shown that there are inherent differences in the number and intensity of vibrational modes observed in pump−probe signals compared with those in resonance Raman spectra.[22] The two measurements are complementary but not equivalent.

The most prominent vibrational modes in the spinach and poplar plastocyanin wavelength-integrated pump−probe spectra are at 372 and 385 cm^{-1}, respectively (Figures 3b and 5b). The fairly long LPSVD decay times (1.44 and 2.52 ps) for these features indicate that they are ground-state vibrational modes. Consistent with these observations, Loppnow and Fraga observed Raman frequencies at 374 and 383 cm^{-1} for spinach plastocyanin and 375 and 382 cm^{-1} for poplar plastocyanin.[20b] Since the resonance Raman spectra show at least eight modes between 260 and 760 cm^{-1}, it seems from these wavelength-integrated measurements that the pump−probe technique is detecting only a portion of the nuclear motion that is known to be coupled to plastocyanin's charge-transfer transition. However, several researchers have observed that the oscillatory character of pump−probe signals depends strongly on the wavelength of the probe.[30] Probing to the red of the pump center frequency often reveals oscillations that are phase-shifted by 180° relative to those observed by probing to the blue. This is because probing higher or lower in energy than the pump center frequency tends to access the excited-state wave packet when it is at one of its two classical turning points on the upper surface. The turning points are always 180° out of phase with each other. When broad-bandwidth optical pulses are used to pump and probe a vibrational mode with a fairly small electron−nuclear coupling (i.e., excited-state displacement), the pulses can have enough spectral width to simultaneously probe both turning points of the excited-state potential. Thus, the probe can contain antiphased oscillations for some vibrational frequencies that cancel out in the wavelength-integrated signal. For this reason, wavelength-resolved pump−probe measurements can give additional vibrational information beyond that found in wavelength-integrated signals.

The wavelength-resolved signals for spinach plastocyanin (Figure 4a) display the effects described in the previous paragraph. Detection of the pump−probe signal at 750 nm reveals oscillations that are out of phase with those detected at 800 nm (the laser center frequency is 770 nm). These oscillations are of much greater amplitude than those in the wavelength-integrated signal, and as shown in the Fourier spectrum of the 750-nm signal (Figure 4b), new frequencies are present. The spectrum still has a peak at 372 cm^{-1}, but it is overshadowed by a broad band with a maximum at 510 cm^{-1}. The assignment of this feature is not apparent, since a mode of this frequency has not been seen in resonance Raman spectra of plastocyanin. One possible source for this mode could be an active site vibration that is coupled to the d → d transitions but not to the charge-transfer transition. This does not seem likely for two reasons. First, since the d → d transitions obtain their oscillator strength by mixing with the charge-transfer band,[8] it is expected that their Raman excitation profiles will be similar. Second, a normal-coordinate analysis of a 169-atom model of plastocyanin by Urushiyama and Tobari did not show any modes of ~500 cm^{-1} to be coupled to active site atoms.[31] Another possibility is that the doubled Cu−N(histidine) stretch, which has a frequency of 263 cm^{-1} (ref 20b), is being observed. In a pump−probe measurement, a vibrational mode can be observed at twice its fundamental frequency if the probe is resonant when the moving, excited-state wave packet is at the minimum of the excited-state well, but off-resonant when the wave packet is at either of the classical turning points. In this case, the wave packet is probed twice per period and frequency doubling is observed.[30] However, this is probably not the source of the 510 cm^{-1} mode in these data because the oscillation is observed in antiphased components of the probe that are to the red or the blue of the probe center frequency. In addition, our wavelength-resolved measurements on spinach plastocyanin detected a mode of around 250 cm^{-1} that has lifetime of >500 fs (Table 1). This frequency, which probably corresponds to the Cu−N(histidine) stretch, is most likely not the result of excited-state wave packet motion because the lifetime of this mode is significantly greater than that of the excited state. A third possibility for this new oscillation results from a nonresonant solvent contribution to the signal. This is not likely, since water (easily the highest-concentration component of the solvent) does not have any peaks in its Raman spectrum[32] near 500 cm^{-1} and the solvent-blank data of Figure 3b (and wavelength-resolved data not shown here) do not exhibit any oscillatory behavior.

A possible assignment for this new mode in spinach plastocyanin, consistent with current resonance Raman data, would be as an excited-state vibrational frequency. The LPSVD time constant for the 510 cm^{-1} mode is 260 fs, almost identical to the excited-state lifetime. In contrast to this, the known ground-state mode at 372 cm^{-1} has a time constant of over a picosecond. Peaks in resonance Raman spectra correspond only to ground-state modes and thus give no direct indication if frequency shifts occur on the excited-state surface.[21] If this newly observed feature is an excited-state mode, one is immediately faced with the question of the source for the frequency increase. A simple explanation would involve one of plastocyanin's six prominent ground-state modes being promoted upon excitation to a potential surface that has a greater effective frequency than the ground-state surface. In the absence of coupling to other nuclear or electronic degrees of freedom, such a "hardening" of the potential surface (through increases in either harmonic or anharmonic contributions) is unlikely. This is because optical excitation involves the promotion of an electron to an orbital that has less bonding character than that electron's ground-state orbital[33] and thus induces a shallower nuclear potential surface in the excited state.

One way a ground-state mode could be upshifted in frequency in the excited state can be envisioned by noting that the ground and excited states involved in the pump−probe measurements must be fairly strongly coupled. As explained above, the rapid decay of the ground-state bleach implies a significant interaction between these surfaces. Figure 8 is a schematic diagram

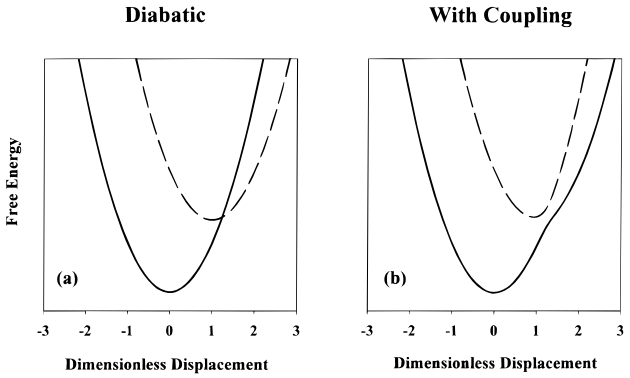

Figure 8. (a) Two displaced, diabatic free-energy surfaces plotted as a function of a generic nuclear coordinate that could represent two electronic levels and an associated harmonic vibrational mode. (b) Free-energy surfaces after a coupling has been added and the Hamiltonian is diagonalized. The avoided crossing distorts the upper surface such that it effectively has a higher frequency (although it is no longer harmonic).

showing the general effect of a coupling on two displaced, parabolic, electronic free-energy surfaces plotted as a function of a generic nuclear coordinate. The diagram on the left (Figure 8a) shows the two surfaces before the coupling is taken into account; they are diabatic and contain a crossing. When a coupling is added and the system Hamiltonian is diagonalized, two orthogonal surfaces are produced (Figure 8b). Note that the avoided crossing significantly distorts the curves from their original shapes. The upper surface becomes more sharply curved, and, although it is no longer harmonic, it will clearly have a higher effective frequency than the diabatic excited-state surface. Although this situation is consistent with the rapid excited-state decay observed in plastocyanin, it is inconsistent with the 180° phase shift observed in the wavelength-resolved pump−probe measurements. In the diabatic view, the lower surface intersects with the upper surface near its minimum. This implies such a large displacement of the upper surface that, if this was a reasonable way to model dynamics in plastocyanin, the 15-fs optical pulses would not have enough bandwidth to probe the excited-state wave packet on both sides of the potential well in an equal fashion. Furthermore, the magnitude of the dimensionless displacement and electronic coupling matrix element (∼2000 cm^{-1}) required to obtain these curves, which would yield a 10−20% increase in vibrational frequency, are unreasonably large. Therefore, strong electronic coupling between the ground and excited states is unlikely to account for an increase in a vibrational frequency.

Duschinsky Rotation. A more likely source for a frequency increase in the excited state can be found by considering the phenomenon of Duschinsky rotation.[34] Duschinsky rotation occurs when geometry and/or force-constant differences between ground and excited structures require the excited-state coordinate system to be rotated with respect to the ground-state in order to maintain normal coordinates. Excited-state normal coordinates are formed from linear combinations of ground-state coordinates of the same symmetry. The frequencies of the resulting excited-state modes can be significantly different from the corresponding ground-state frequencies. For example, Hemley et al. reported that a 1638 cm^{-1} ground-state vibrational frequency of 1,3-butadiene increases to 1670 cm^{-1} in the $1^1B_u^+$ excited state through Duschinsky mixing with another mode.[35] This effect is general and must be taken into account in a complete description of a molecule's absorption, fluorescence, and resonance Raman spectra.[36] One indication of significant Duschinsky mixing in a molecule is the presence of strong combination bands in its resonance Raman spectrum.[37] It is important to point out that while Duschinsky rotation tends to increase the cross section for excitation of combinations of ground-state modes in the Raman process, the excited-state vibrational frequencies are not required to be formed from linear combinations of ground-state frequencies.

If significant Duschinsky rotation occurs among spinach plastocyanin's Raman-active modes that contain the Cu−S(cysteine) stretch, that is, the six modes in the range 370−480 cm^{-1} (refs 16 and 20a), it is conceivable that upon excitation a mode of around 500 cm^{-1} could exist on the excited-state surface with appreciable displacement. As an example of how this might occur, consider the possibility of Duschinsky mixing between plastocyanin's 421 and 473 cm^{-1} ground-state modes.[20a] For purposes of illustration, assume that in the excited-state appropriate geometry changes occur to mix these two ground-state modes such that one mode shifts down in frequency by 27 cm^{-1} to 394 cm^{-1} while the other shifts up by the same amount to 500 cm^{-1}. A typical value of the Duschinsky rotation angle θ_D required to transform the ground-state normal-coordinate system to the excited state might be 15°. Using these values, one can calculate ground and excited potential-energy surfaces for this two-mode system in order to form a basic picture of how Duschinsky rotation could manifest itself in plastocyanin. Equation 1 describes how the ground-state normal coordinates $\mathbf{q}_g$ can be transformed into the excited-state normal coordinates $\mathbf{q}_e$:[36]

$$\mathbf{q}_e = \mathbf{S}\mathbf{q}_g + \mathbf{D} \tag{1}$$

Here, **S** is the rotation matrix characterized by the angle θ_D and **D** is a vector containing the displacements of the excited-state modes. For a two-mode system, **S** is written as

$$\mathbf{S} = \begin{bmatrix} \cos\theta_D & \sin\theta_D \\ -\sin\theta_D & \cos\theta_D \end{bmatrix} \tag{2}$$

For simplicity of presentation, it is assumed that the two components of **D** are equal. Figure 9 shows the ground (part a) and excited (part b) potential-energy surfaces calculated with eq 1. Both surfaces are plotted as a function of the ground-state normal coordinates. Note that the contours of the excited-state surface are more elliptical than the ground state, indicative of the greater frequency difference between the two modes in the excited state. Also note that, in the excited state, a motion with an initial velocity along either of the ground-state normal coordinates will acquire a component parallel to the other coordinate. An important consequence of this is that, in the pump−probe process, some wave-packet motion will be induced along a mode with no excited-state displacement if it undergoes Duschinsky-type mixing with another mode. Since small-amplitude wave packet motion is often not observed in broad band, wavelength-integrated pump−probe measurements (vida supra and ref 30), this scenario could provide an explanation as to why the 510 cm^{-1} mode is only observed in wavelength-resolved measurements.

A strong piece of evidence in support of the possibility of a Duschinsky effect in plastocyanin is the fact that this protein's resonance Raman spectrum shows a broad and intense combination band centered at ∼800 cm^{-1}, apparently involving most if not all combinations of the group of modes around 400 cm^{-1}.[17−20] Blair et al.[17a] took this as evidence of "extreme" Duschinsky rotation in the excited state of plastocyanin. Therefore, this effect provides a possible explanation for plastocyanin having an excited-state mode of ∼500 cm^{-1}. We

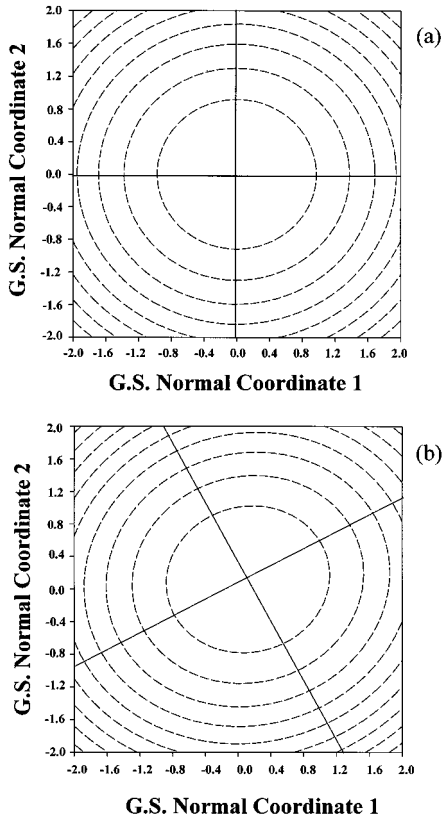

Figure 9. Contour plots of model potential-energy surfaces for a two-mode system demonstrating Duschinsky rotation and excited-state displacement. In the ground state (a), the frequencies of the modes are 421 and 473 cm^{-1}. In the excited state (b), it is assumed that appropriate geometry changes have taken place in order to cause the frequencies to shift to 394 and 500 cm^{-1}. The Duschinsky rotation angle is taken to be 15°. Both surfaces are plotted as a function of the ground-state (G.S.) dimensionless normal coordinates. The perpendicular lines overlayed on the contours are the axes of the normal coordinates on each surface.

have performed nonlinear response-function simulations of the wavelength-integrated and wavelength-resolved data presented here. However, these simulations are not explicitly consistent with a Duschinsky effect in that only a single-mode coordinate was examined. Further simulations are in progress.

Connection to Structure. The observation of an intense mode of ~500 cm^{-1} in a pump−probe spectrum of spinach plastocyanin raises the question as to whether this occurrence is general to blue copper proteins. Since the basic structure of the blue copper active site and certain features in resonance Raman spectra are highly conserved among different proteins and species,[6,17a] it might be expected that other aspects related to the structure and dynamics of blue copper proteins will be conserved as well. The Fourier spectrum associated with the pump−probe measurement of ceruloplasmin (750-nm detection) shows intense modes at 361, 430, and 506 cm^{-1} (Figure 7b). The first two modes can be associated with frequencies observed in resonance Raman measurements,[17a] but the 506 cm^{-1} feature is unique. Like the analogous mode in spinach plastocyanin, this oscillation has an LPSVD time constant of about the value of the excited-state lifetime (250 fs). Since human ceruloplasmin and spinach plastocyanin differ widely in terms of size, overall structure, and biological function, this suggests that this previously unobserved mode may be a "universal" characteristic of blue copper proteins. However, the wavelength-resolved pump−probe spectrum for poplar plastocyanin does not show any peaks near 500 cm^{-1} (Figure 6b). This seems strange, since spinach and poplar plastocyanin are clearly much more similar than plastocyanin and ceruloplasmin.

There are some indications, however, that significant structural and spectroscopic differences could exist between these two plastocyanins. Although the structure of poplar plastocyanin is well characterized by X-ray crystallography,[15] a complete high-resolution structure has not been reported for the spinach species because of difficulties with crystallization. Loppnow and Fraga detected significant differences between these two plastocyanins in terms of the strengths of coupling of modes to the charge-transfer excitation.[20b] They performed electrostatic calculations on both proteins that suggested that these differences can be explained by the coupling of active-site internal coordinates to neighboring amino acid residues that differ between the two species. Therefore, there seem to be structural differences that might account for the observation of different pump−probe dynamics in these two proteins.

All pump−probe spectra we have obtained for these blue copper proteins contain peaks in the range 35−55 cm^{-1}. It is tempting to assign these low-frequency features to protein "phonon" modes that are coupled to the optical excitation. The existence of such modes would directly implicate the protein matrix in relaxation processes resulting from a perturbation at the active site and thus could play an important role in the biological electron-transfer process. However, there are other possible sources for these peaks, and it would be premature to make a definitive assignment. These spectral features might be attributed to difference frequencies of higher-energy vibrations, including ones involved in Duschinksy-mixing in the excited state. It is known that the resonance Raman cross sections for combination bands in these proteins are fairly high,[17a] so it might be expected that difference frequencies will have similar intensities. Unfortunately, resonance Raman measurements of small enough frequency shifts to access this region of the spectrum are difficult because of Rayleigh scattering of the excitation source. These low-frequency features could also be artifacts due to nonexponential decays of the pump−probe signals. It was necessary to subtract exponential fits from the time-domain data prior to the Fourier transformation. Imperfect fits could produce low-frequency peaks in the resulting spectra. Still, biexponential fits to the data gave identical results. More extensive measurements on wild-type and mutant proteins will have to be made to determine the origin, physical or otherwise, of these low-frequency peaks.

V. Conclusions

The results of the present pump−probe measurements of spinach plastocyanin, poplar plastocyanin, and human ceruloplasmin allow some general observations to be made on electronic and nuclear dynamics in the active sites of blue copper proteins. The decay of the pump-induced ground-state bleach with a lifetime of 230−300 fs indicates that a fairly strong coupling exists between the ground and excited states accessed in this study. This result is in quantitative agreement with the measurements made by Beck and co-workers.[23] The present study detected vibrational coherences at frequencies corresponding to modes involving the Cu−S(cysteine) stretch. This observation is consistent with conclusions drawn from resonance Raman spectra that this bond undergoes significant distortion upon optical excitation of the blue copper protein.[17−20] A new mode at ~500 cm^{-1} is observed in spinach plastocyanin and ceruloplasmin, which is attributed to an excited-state mode. This assignment indicates that nuclear dynamics on excited-state surfaces are likely to be somewhat different than ground-state

dynamics. These differences could be the result of Duschinsky rotation among vibrational degrees of freedom in the excited state.

These results imply that, to simulate physiological electronic transfer, it will probably not be possible to model a blue copper protein as a simple two-level electronic system coupled to a single harmonic vibrational mode. The five copper d levels and the charge-transfer orbital from the cysteine sulfur ligand may all be coupled to each other. Although the Cu−S(cysteine) bond appears to be the dominant mode coupled to the optical excitation, this internal coordinate is distributed among at least six normal modes. Also, Duschinsky rotation may invalidate the notion of a one-to-one correspondence between ground- and excited-state vibrational modes. Therefore, it is essential to model the reaction coordinates for excitation and nonradiative decay as a combination of several nuclear degrees of freedom.

Further work will be necessary in order to resolve the issues raised by this study and to make contact with theory and simulation results. An especially useful measurement would involve pumping and probing plastocyanin's charge-transfer transition with pulses short enough to resolve the nuclear motion coupled to the excitation. This would provide experimental data for direct comparison with the molecular dynamics simulations performed by Ungar et al.[16] Such a measurement would also aid in ongoing efforts to perform quantum mechanical simulations of return electron transfer in optically excited blue copper proteins.[38] It would be especially interesting to find out if a 500 cm^{-1} mode is observed as a result of the charge-transfer excitation. To directly map out couplings between the excited states of the blue copper active site, it would be useful to pump the charge-transfer band at ∼600 nm and probe the d → d band at ∼770 nm. These measurements, which are in progress, will allow much more complete characterization of nuclear and electronic dynamics in the states that participate in the biological electronic transfer function of these proteins.

Acknowledgment. We are grateful to Professor Greg Voth and Dr. Lowell Ungar for helpful discussions. We thank Professor Glen Loppnow for providing the poplar plastocyanin sample, Professor Warren Beck for providing ref 23 prior to publication, and Professor Ponzy Lu and his group for providing use of their centrifuge and advice on the isolation of spinach plastocyanin. We thank the NIH (GM 57768-01) and the NSF National Young Investigator program (CHE-9357424) for financial support. N.F.S. also acknowledges the Arnold and Mabel Beckman, David and Lucille Packard, Alfred P. Sloan, and Camille and Henry Dreyfus foundations for fellowships and awards supporting this research.

References and Notes

(1) (a) Winkler, J. R.; Gray, H. B. *Chem. Rev.* **1992**, *92*, 369. (b) McLendon, G.; Hake, R. *Chem. Rev.* **1992**, *92*, 481.

(2) (a) Moser, C. C.; Keske, J. M.; Warncke, K.; Farid, R. S.; Dutton, P. L. *Nature* **1992**, *355*, 796. (b) Moser, C. C.; Page, C. C.; Farid, R. S.; Dutton, P. L. *J. Bioenerg. Biomembr., Proc. Int. Symp.* **1995**, *27*, 263.

(3) (a) Miller, J. R.; Calcaterra, L. T.; Closs, G. L. *J. Am. Chem. Soc*. **1984**, *106*, 3047. (b) Closs, G. L.; Miller, J. R. *Science* **1988**, *240*, 440.

(4) (a) Marcus, R. A. *J. Chem. Phys*. **1956**, *24*, 966. (b) Marcus, R. A.; Sutin, N. *Biochim. Biophys. Acta* **1985**, *811*, 265.

(5) Myers, A. B. *Chem. Rev.* **1996**, *96*, 911.

(6) Sykes, A. G. *Adv. Inorg. Chem*. **1991**, *36*, 377.

(7) Solomon, E. I.; Baldwin, M. J.; Lowery, M. D. *Chem. Rev*. **1992**, *92*, 521.

(8) Gewirth, A. A.; Solomon, E. I. *J. Am. Chem. Soc*. **1988**, *110*, 3811.

(9) Guckert, J. A.; Lowery, M. D.; Solomon, E. I. *J. Am. Chem. Soc*. **1995**, *117*, 2817.

(10) Larsson, S.; Broo, A.; Sjölin, L. *J. Phys. Chem*. **1995**, *99*, 4860.

(11) Solomon, E. I.; Hare, J. W.; Dooley, D. M.; Dawson, J. H.; Stephens, P. J.; Gray, H. B. *J. Am. Chem. Soc*. **1980**, *102*, 168.

(12) Redinbo, M. R.; Yeates, T. O.; Merchant, S. *J. Bioenerg. Biomembr., Proc. Int. Symp.* **1994**, *26*, 49.

(13) (a) Takahashi, N.; Ortel, T. L.; Putnam, F. W. *Proc. Natl. Acad. Sci. U.S.A.* **1984**, *81*, 390. (b) Zaitseva, I.; Zaitsev, V.; Card, G.; Moshkov, K.; Bax, B.; Ralph, A.; Lindley, P. *J. Biol. Inorg. Chem*. **1996**, *1*, 15.

(14) Kaplan, J.; O'Halloran, T. V. *Science* **1996**, *271*, 1510.

(15) Guss, J. M.; Bartunik, H. D.; Freeman, H. C. *Acta Crystallogr*. **1992**, *B48*, 790.

(16) Ungar, L. W.; Scherer, N. F.; Voth, G. A. *Biophys. J*. **1997**, *72*, 5.

(17) (a) Blair, D. F.; Campbell, G. W.; Schoonover, J. R.; Chan, S. I.; Gray, H. B.; Malmstrom, B. G.; Pecht, I.; Swanson, B. I.; Woodruff, W. H.; Cho, W. K.; English, A. M.; Fry, H. A.; Lum, V.; Norton, K. A. *J. Am. Chem Soc*. **1985**, *107*, 5755. (b) Woodruff, W. H.; Dyer, R. B.; Schoonover, J. R. *Biological Applications of Raman Spectroscopy*; Spiro, T. G, Ed.; Wiley: New York, 1988; Vol. 3, pp 413−438.

(18) Qiu, D.; Dong, S.; Ybe, J. A.; Hecht, M. H.; Spiro, T. G. *J. Am. Chem. Soc*. **1995**, *117*, 6443.

(19) (a) Han, J.; Adman, E. T.; Beppu, T.; Codd, R.; Freeman, H. C.; Huq, L.; Loehr, T. M.; Sanders-Loehr, J. *Biochemistry* **1991**, *30*, 10904. (b) Andrew, C. R.; Sanders-Loehr, J. *Acc. Chem. Res*. **1996**, *29*, 365.

(20) (a) Fraga, E.; Webb, M. A.; Loppnow, G. R. *J. Phys. Chem*. **1996**, *100*, 3278. (b) Loppnow, G. R.; Fraga, E. *J. Am. Chem. Soc*. **1997**, *119*, 896.

(21) Myers, A. B.; Mathies, R. A. *Biological Applications of Raman Spectroscopy*; Spiro, T. G, Ed.; Wiley: New York, 1988; Vol. 2, pp 1−58.

(22) Johnson, A. E.; Myers, A. B. *J. Chem. Phys*. **1996**, *104*, 2497.

(23) Edington, M. D.; Diffey, W. M.; Doria, W. J.; Riter, R. E.; Beck, W. F. *Chem. Phys. Lett*. **1997**, *275*, 119.

(24) Asaki, M. T.; Huang, C.-P.; Garvey, D.; Zhou, J.; Kapteyn, H. C.; Murnane, M. M. *Opt. Lett*. **1993**, *18*, 977.

(25) (a) Arnett, D. C.; Horn, M. A.; Scherer, N. F. *J. Opt. Soc. Am. B*., submitted. (b) Horn, M. A.; Arnett, D. C.; Scherer, N. F. *Proc. SPIE*, in press.

(26) (a) Scherer, N. F.; Book, L. D.; Ungar, L. W.; Arnett, D. C.; Hu, H.; Voth, G. A. *Ultrafast Phenomena X*; Barabara, P. F., Fujimoto, J. G., Knox, W. H., Zinth, W., Eds.; Springer-Verlag: Berlin, 1996; pp 361−362. (b) Arnett, D. C.; Book, L. D.; Ungar, L. W.; Hu, H.; Voth, G. A.; Scherer, N. F. *Fifteenth International Conference on Raman Spectroscopy*; Asher, S. A., Stein, P. Eds.; Wiley: New York, 1996; pp 314−315. (c) Book, L. D.; Ungar, L. W.; Arnett, D. C.; Hu, H.; Voth, G. A.; Scherer, N. F. *QELS '97*; Optical Society of America: Washington, DC, 1997; p 163.

(27) Morand, L.; Krogmann, D. *Biochim. Biophys. Acta* **1993**, *1141*, 105.

(28) Barkhuisjen, H.; de Beer, R.; Bovee, W. M. M. J.; van Ormondt, D. *J. Magn. Reson*. **1985**, *61*, 465.

(29) (a) Horng, M. L.; Gardecki, J. A.; Papazyan, A.; Maroncelli, M. *J. Phys. Chem*. **1995**, *99*, 17311. (b) Kumar, P. V.; Maroncelli, M. *J. Chem. Phys*. **1995**, *103*, 3038.

(30) (a) Pollard, W. T.; Dexheimer, S. L.; Wang, Q.; Peteanu, L. A.; Shank, C. V.; Mathies, R. A. *J. Phys. Chem*. **1992**, *96*, 6147. (b) Scherer, N. F.; Jonas, D. M.; Fleming, G. R. *J. Chem. Phys*. **1993**, *99*, 153. (c) Jonas, D. M.; Bradforth, S. E.; Passino, S. A.; Fleming, G. R. *J. Phys. Chem*. **1995**, *99*, 2594.

(31) Urushiyama, A.; Tobari, J. *Bull. Chem. Soc. Jpn*. **1990**, *63*, 1563.

(32) Castner, E. W.; Chang, Y. J.; Chu, Y. C.; Walrafen, G. E. *J. Chem. Phys*. **1995**, *102*, 653.

(33) Herzberg, G. *Molecular Spectra and Molecular Structure. III. Electronic Spectra and Electronic Structure of Polyatomic Molecules*; Van Nostrand Reinhold Co.: New York, 1966.

(34) Duschinskii, F. *Acta Physicochim. URSS* **1937**, *7*, 551.

(35) Hemley, R. J.; Dawson, J. I.; Vaida, V. *J. Chem. Phys*. **1983**, *78*, 2915.

(36) (a) Yan, Y. J.; Mukamel, S. *J. Chem. Phys*. **1986**, *85*, 5908. (b) Tannor, D. J.; Heller, E. J. *J. Chem. Phys*. **1982**, *77*, 202.

(37) Morris, D. E.; Woodruff, W. H. *J. Phys. Chem*. **1985**, *89*, 5795.

(38) Ungar, L. W.; Voth, G. A. Work in progress.